Unveiling the Reaction Mechanism of Sb_2S_3-Co_9S_8/NC Anode for High-Performance Lithium-Ion Batteries

Guanxia Ke [a #], Xiaochao Wu [a #], Huanhui Chen [a, b #], Wanqing Li [a], Shuang Fan [a], Hongwei Mi [a] *, Yongliang Li [a], Qianling Zhang [a], Chuanxin He [a], Xiangzhong Ren [a] *

[a] *College of Chemistry and Environmental Engineering, International Joint Research Center for Molecular Science, Shenzhen University, Shenzhen, Guangdong 518060, P.R. China*

[b] *Shenzhen Engineering Laboratory of Flexible Transparent Conductive Films, School of Materials Science and Engineering, Harbin Institute of Technology, Shenzhen 518055, P.R. China*

Corresponding author:

Xiangzhong Ren, E-mail: renxz@szu.edu.cn, Tel/Fax: +86-755-26558134

Hongwei Mi, E-mail: milia807@szu.edu.cn, Tel/Fax: +86-755-26538657

# These authors contributed equally to this work and should be considered as co-first authors.

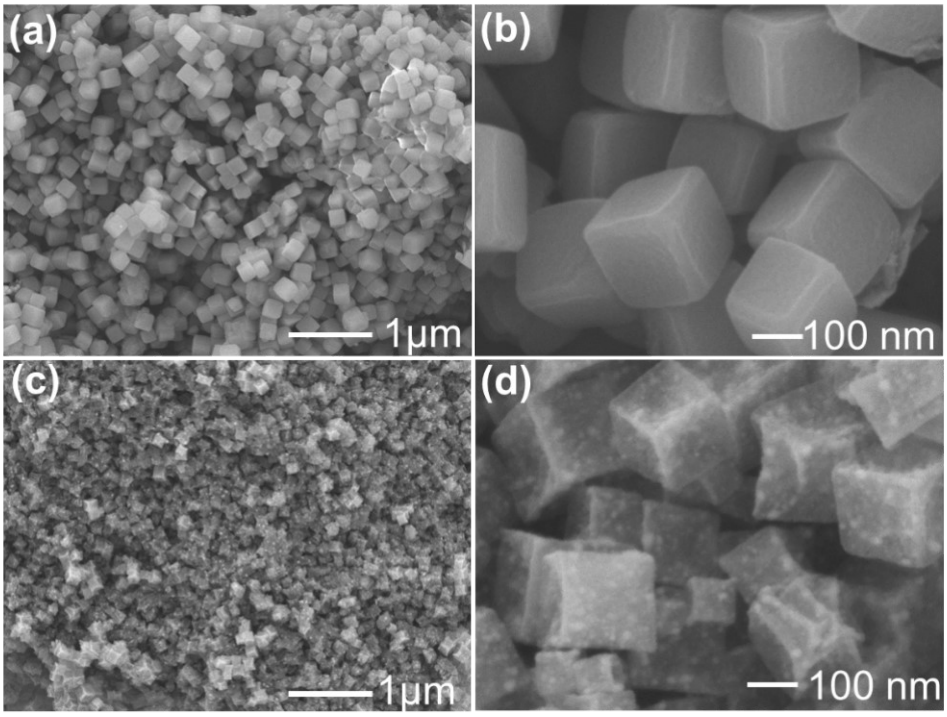

Fig. S1. SEM images of (a-b) the ZIF-67sample and (c-d) the Co/NC sample.

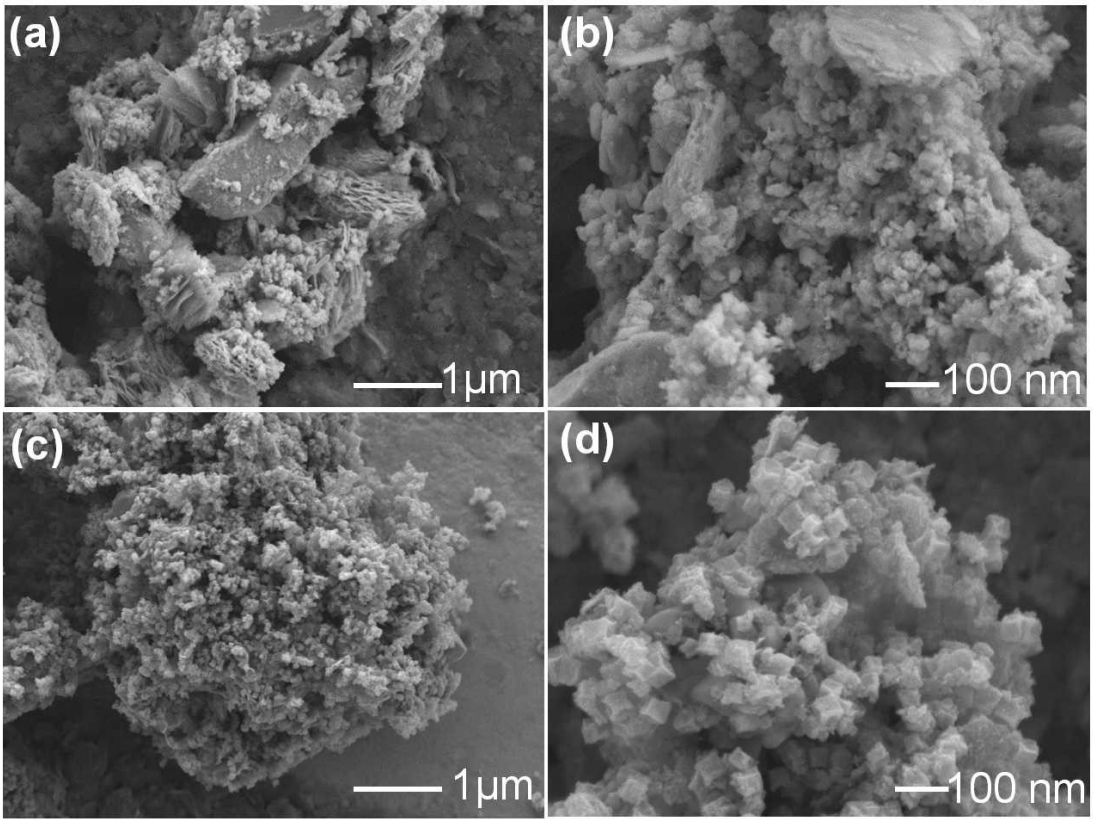

Fig. S2. SEM images of (a-b) the Sb_2S_3 sample and (c-d) the Co_9S_8/NC sample.

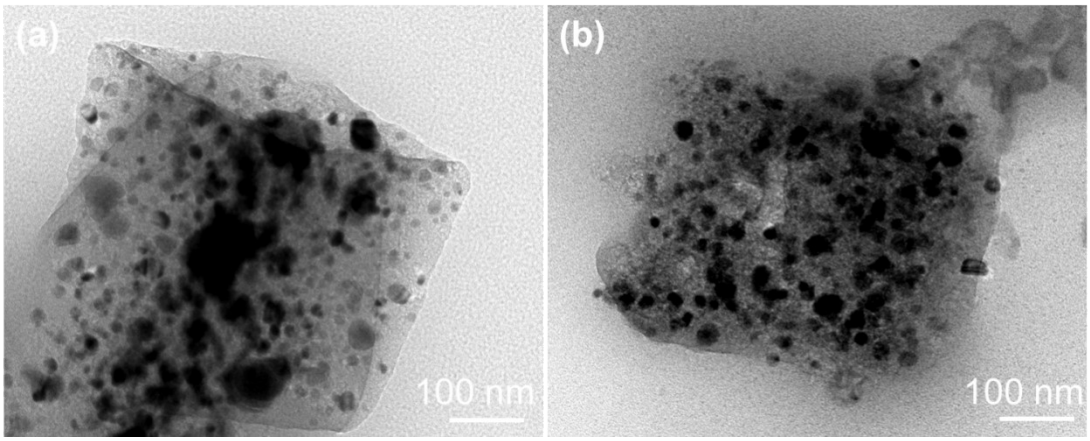

Fig. S3. TEM images of (a) the Co/NC sample and (b) the Co_9S_8/NC sample.

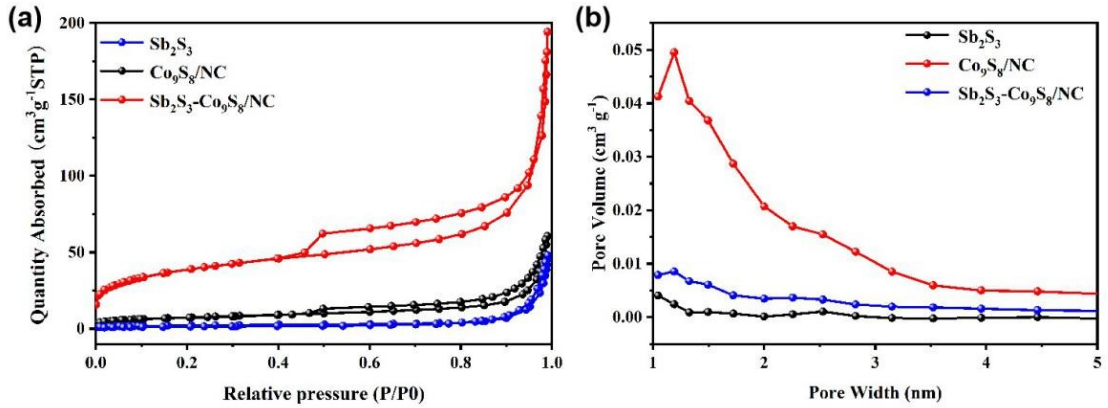

Fig. S4. (a)Nitrogen adsorption–desorption isotherm curves and (b) pore size distributions of Sb_2S_3, Co_9S_8/NC and Sb_2S_3-Co_9S_8/NC samples.

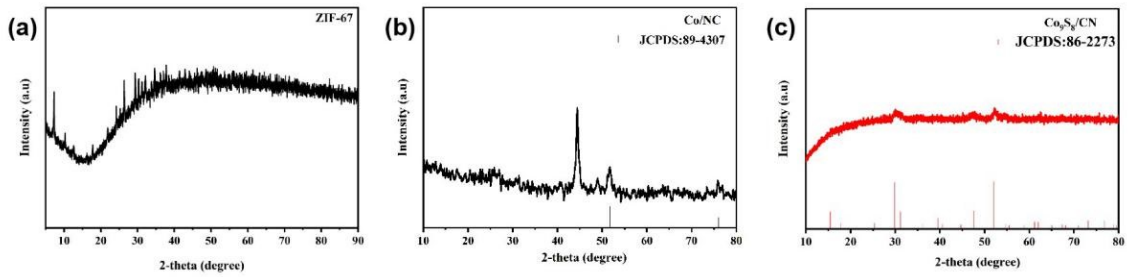

Fig. S5. XRD of (a) ZIF-67 sample, (b) Co/NC sample and (c) Co_9S_8/NC sample.

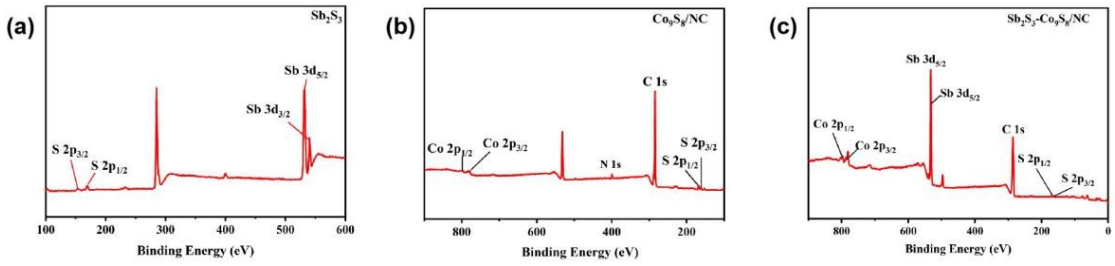

Fig. S6. XPS spectra of (a) the Sb_2S_3, (b) Co_9S_8/NC and (c) Sb_2S_3-Co_9S_8/NC.

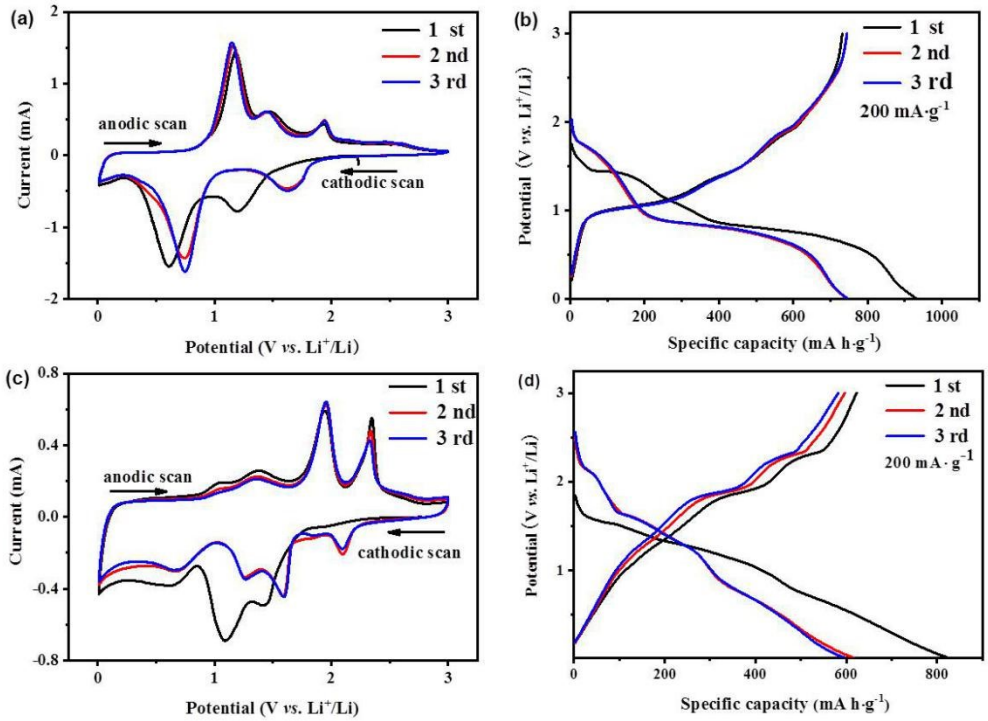

Fig. S7. (a)(c) CV curves of Sb_2S_3 and Co_9S_8/NC in the potential range at 0.01-3 V at 0.2 $mV \cdot s^{-1}$; (b)(d) the discharge–charge curves of the Sb_2S_3 and Co_9S_8/NC at a current density of 0.2 $A \cdot g^{-1}$.

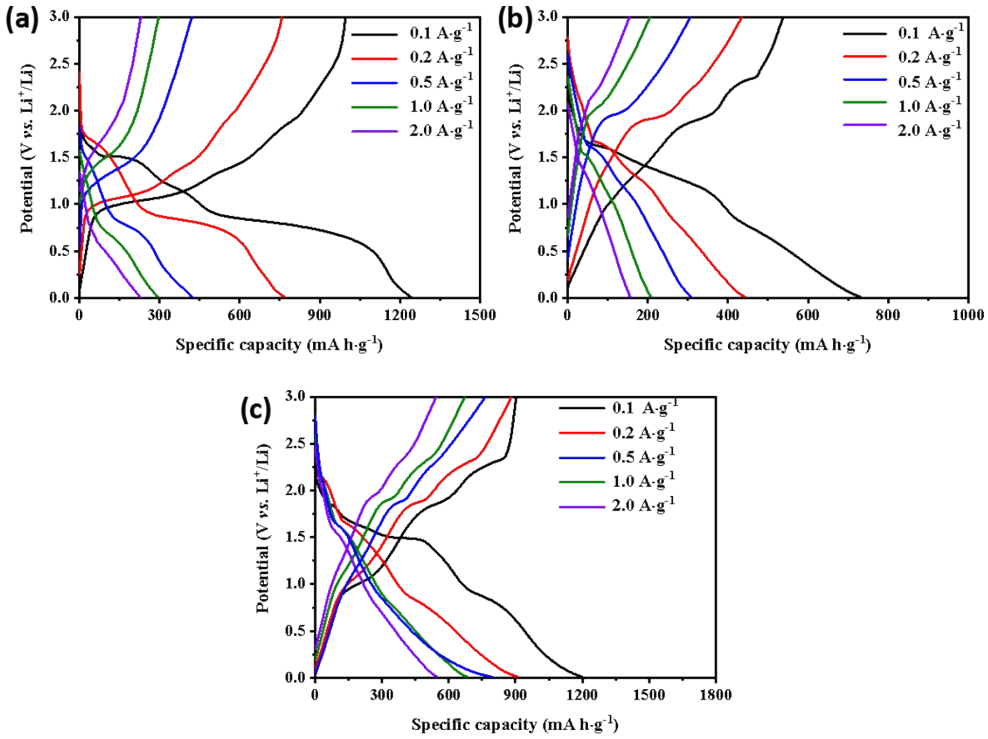

Fig. S8. The Charge / Discharge curves of Sb_2S_3(a), Co_9S_8/NC(b) and Sb_2S_3-Co_9S_8/NC at various rates.

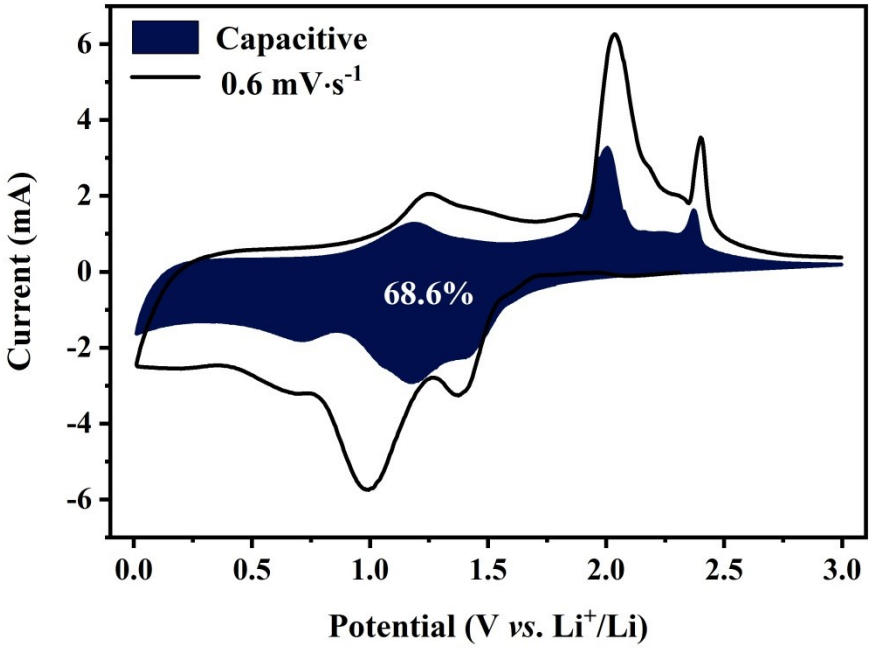

Fig. S9. CV curve with the pseudocapacitive contribution of Sb_2S_3-Co_9S_8/NC at 0.6 mV·s $^{-1}$.

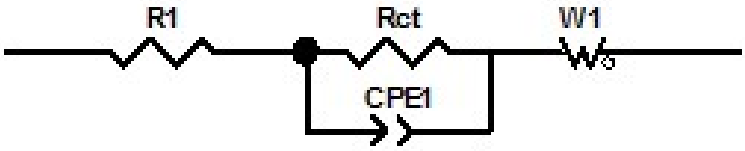

Fig. S10. The equivalent circuit of the samples.

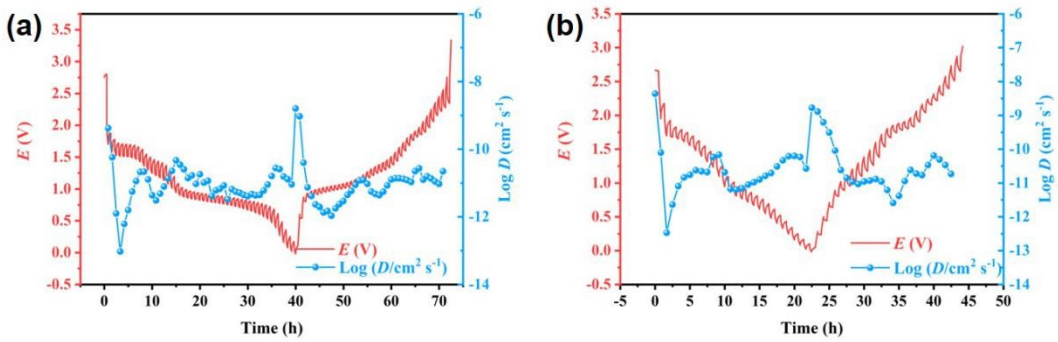

Fig. S11. GITT and DLi^+ curves of (a) Sb_2S_3 electrode and (b) Co_9S_8/NC electrode.

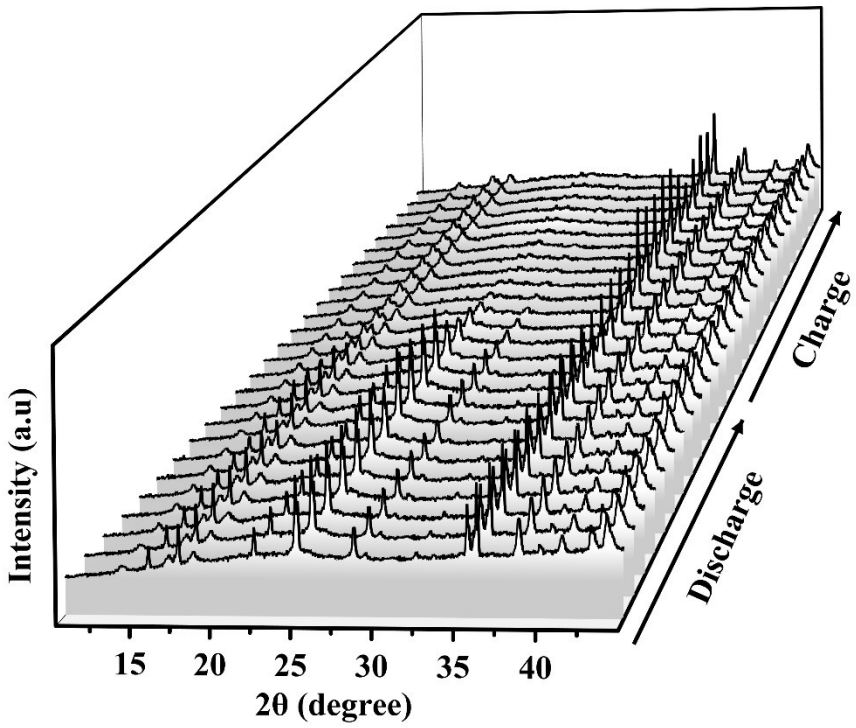

Fig. S12. 3D waterfall chart of Sb_2S_3-Co_9S_8/NC electrodes during the first cycle.

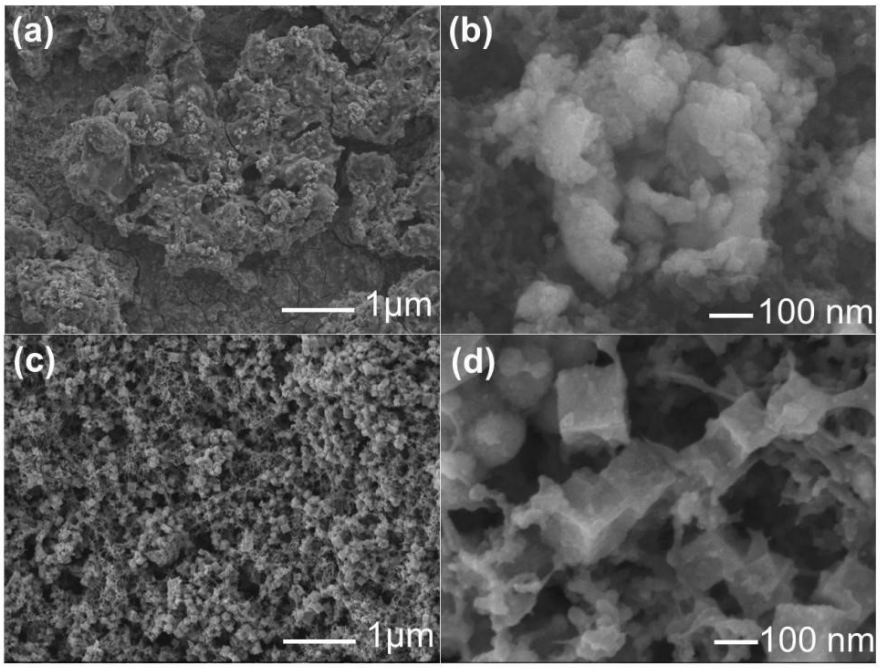

Fig. S13. SEM images of Sb_2S_3 (a, b) and Sb_2S_3-Co_9S_8/NC (c, d) at different magnifications after 100 cycles.

Table S1. Element content for Sb_2S_3-Co_9S_8/NC obtained from ICP analysis.

Mass(g)	Element	Elemental content ($mg \cdot L^{-1}$)	Weight (%)
0.0344	Co	6.37	18.52
0.0344	S	6.43	18.68
0.0344	Sb	3.07	8.92

Table. S2. Comparison of the electrochemical lithium storage performance of the Sb_2S_3-Co_9S_8/NC electrodes with the literature data.

Materials	Current density ($mA \cdot g^{-1}$)	cycle number (cycles)	Reversible Capacity ($mA\ h \cdot g^{-1}$)	reference
Sb_2S_3-Co_9S_8/NC-2	**2000**	**900**	**616**	**This work**
Sb_2S_3/EG-S	5000	100	548	1
Sb_2S_3/CS	200	200	566	2
Co_9S_8@MoS_2	1000	300	1048	3
Co_9S_8/ZnS@NC	1000	300	411	4
hollow core–shell ZnCoS@Co_9S_8/NC	2000	400	1095	5
NiS_2@CoS_2@C@C	1000	100	680	6
Bi_2S_3@Co_9S_8 CHPs	500	800	595	7
Co_9S_8@MPCNF-15	200	200	654	8
$Co_{1-x}S$/NC@MoS_2/C	100	150	910	9
$Co_{1-x}S$/NCS	200	100	796	10

CoS_2-in-wall-NCSs	200	500	1165	11
Sb_2S_3 hollow microspheres	1000	100	600	12
2D Sb_2S_3	2000	10	750	13

References

1. Wang, S.; Cheng, Y.; Xue, H.; Liu, W.; Yi, Z.; Chang, L.; Wang, L. Multifunctional sulfur-mediated strategy enabling fast-charging Sb_2S_3 micro-package anode for lithium-ion storage. *Journal of Materials Chemisry A* **2021**, 9**,** 7838-7847.
2. Xie, J.; Xia, J.; Yuan, Y.; Liu, L.; Zhang, Y.; Nie, S.; Yan, H. Sb_2S_3 embedded in carbon–silicon oxide nanofibers as high-performance anode materials for lithium-ion and sodium-ion batteries. *Journal Power Sources* **2019**, 435, 226762.
3. Yang, K.; Mei, T.; Chen, Z.; Xiong, M.; Wang, X.; Wang, J.; Li, J.; Yu, L.; Qian, J.; Wang, X. Chinese hydrangea lantern-like Co_9S_8@MoS_2 composites with enhanced lithium-ion battery properties. *Nanoscale* **2020**, 12, 3435-3442.
4. Duan, J.; Wang, Y.; Li, H.; Wei, D.; Wen, F.; Zhang, G.; Liu, P.; Li, L.; Zhang, W.; Chen, Z. Bimetal-organic Framework-derived Co_9S_8/ZnS@NC Heterostructures for Superior Lithium-ion Storage. *Chemistry an-Asian Journal* **2020**, 15, 1613-1620.
5. Aslam, M K.; Shah, S. S.; Li, S.; Chen, C. Kinetically controlled synthesis of MOF nanostructures: single-holed hollow core–shell ZnCoS@Co_9S_8/NC for ultra-high performance lithium-ion batteries. *Journal of Materials Chemistry A* **2018**, 6, 14083.
6. Lin, Y.; Qiu, Z.; Li, D.; Ullah, S.; Hai, Y.; Xin, H.; Liao, W.; Yang, B.; Fan, H.; Xu, J.; Zhu, C. NiS_2@CoS_2 nanocrystals encapsulated in N-doped carbon nanocubes for high performance lithium/sodium ion batteries. *Energy Storage Materials* **2018**, 11, 67-74.
7. Huang, Y.; Hu, X.; Li, J;. Zhang, J.; Cai, D.; Sa, B.; Zhan, H.; Wen, Z. Rational construction of heterostructured core-shell Bi_2S_3@Co_9S_8 complex hollow particles toward high-performance Li- and Na-ion storage. *Energy Storage Materials*, **2020**, 29, 121-130.
8. Zhou, X.; Su, K.; Kang, W.; Cheng, B.; Li, Z.; Jiang, Z. Locking metal sulfide nanoparticles in interconnected porous carbon nanofibers with protective macro-porous skin as freestanding anodes for lithium ion batteries. *Chemical Engineering Journal* **2020**, 397, 125271.
9. Wang,Y.; Xie, W.; Li, D.; Han, P.; Shi, L.; Luo, Y.; Cong, G.; Li, C.; Yu J.; Zhu, C.; Xu, J. One-pot synthesis of hierarchical $Co_{1-x}S$/NC@MoS_2/C hollow nanofibers based on one-dimensional metal coordination polymers for enhanced lithium and sodium-ion storage. *Science Bullent* **2020**, 65, 1460-1469.
10. Yang, Z.; Wang, J.; Wu, H.; Kong, F.; Yin, W.; Cheng, H.; Tang, X.; Qian, B.;Tao, S. MOFs derived $Co_{1-x}S$ nanoparticles embedded in N-doped carbon nanosheets with improved electrochemical performance for lithium ion batteries. *Applied Surface Science* **2019**, 479, 693-699.

11. Fang, L.; Zhang, Y.; Guan, Y.; Zhang, H.; Wang, S.; Wang, Y. CoS_2 nanodots trapped within graphitic structured N-doped carbon spheres with efficient performances for lithium storage *Journal Materials Chemistry A* 2018, **6**, 7148-7154.
12. Xie, J.; Liu, L.; Xia, J.; Zhang, Y.; Li, M.; Ouyang, Y.; Nie, S. Wang, X. Template-Free Synthesis of Sb_2S_3 Hollow Microspheres as Anode Materials for Lithium-Ion and Sodium-Ion Batteries. *Nano-Micro Letters* **2018**, 10, 12.
13. Yao, S.; Cui, J.; Deng, Y.; Chong, W.; Kim, J. K. Ultrathin Sb_2S_3 Nanosheet Anodes for Exceptional Pseudocapacitive Contribution to Multi-battery Charge Storage. *Energy Storage Material* **2018**, 20, 36-45.